Ionics (2019) 25:3603–3609
https://doi.org/10.1007/s11581-019-02917-6

ORIGINAL PAPER

Optimize performance of $Li_3V_2(PO_4)_3$/C cathode composite materials through Ti doping

Xumei Cui[1,2] · Tiantian Liu[1]

Received: 17 October 2018 / Revised: 16 January 2019 / Accepted: 6 February 2019 / Published online: 21 February 2019

Abstract

$Li_3V_{2-x}Ti_x(PO_4)_3$/C($x = 0, 0.02, 0.06, 0.08$) composites as cathode material of Li-ion battery with Ti doping was synthesized with carbothermal reduction method, using stearic acid as carbon source. The crystal phase, microstructures, and electrochemical properties of the composites were characterized by XRD, SEM, and electrochemical performance testing. XRD analysis showed that the XRD curve of the Ti-doped composites had no additional reflection curves compared with the XRD curve of the undoped sample, indicating that Ti entered the crystal structure of $Li_3V_2(PO_4)_3$. And the results showed that Ti doping can not only improve the first discharge specific capacity of $Li_3V_2(PO_4)_3$/C composites but also improve its cycle performance at different rate. And $Li_3V_{1.94}Ti_{0.06}(PO_4)_3$/C samples had the best performance with the first discharge capacity of 121.9 $mAhg^{-1}$ and 123.5 $mAhg^{-1}$ with 3.0~4.3 V voltage range and at 0.2 C and 0.5 C rate, respectively. And the capacity retention was 98.69% after 100 cycles at 0.2 C and 98.4% after 15 cycles at 0.5 C, respectively. EIS test results showed that Ti doping affected the charge transfer process and Li-ion transport resistance, and could improve the electrochemical properties of the composites.

Keywords Lithium-ion battery · Lithium vanadium phosphate · Cathode material · Ti doping · Electrochemical properties

Introduction

Recently, with the development of society, unlimited usage of energy source results in energy crisis. The development of lithium-ion batteries (LIBs) with high-specific energy, discharge specific capacity, and excellent cycling stability has become a research focus currently [1–6]. And there are some important issues that need to be resolved before LIBs could be widely used. Since battery performances are mainly determined by cathode materials, much work has been done to develop cathode materials for the lithium ion batteries with excellent performance in new era [1, 2, 5–9]. Monoclinic lithium vanadium phosphate ($Li_3V_2(PO_4)_3$, LVP) is a good cathode candidate material for LIBs owing to its stable structure, high theoretical specific capacity, and good ion diffusion coefficient [10–12]. $Li_3V_2(PO_4)_3$ three-dimensional network structure is composed of VO_6 octahedron and PO_4 tetrahedron by sharing the apex oxygen atoms, and this structure enlarge the space of the insert and extraction of the Li ions [11, 13]. With charge voltage rang of 3.0~4.3 V, its discharge specific capacity can be reached 133 $mAhg^{-1}$, and during the voltage range 3.0~4.8 V, its capacity can be reached 197 $mAhg^{-1}$ [14–16]; at the same time, the three Li ions can be reversibly embedded and escaped from the lattice.

However, some disadvantage exists for $Li_3V_2(PO_4)_3$ with relatively small intrinsic electronic conductivity (10^{-7} Scm^{-1}) and poor cycle stability [17, 18], which enormously restrict its large-scale applications. Therefore, in recent years, giant efforts have been done to optimize the electrochemical properties of $Li_3V_2(PO_4)_3$. Carbon coating and cation doping are the most efficacious methods [16, 19]. Up to now, multifarious carbon resources and lots of cations have been investigated extensively using various preparation routes to optimize the electrochemical performance of $Li_3V_2(PO_4)_3$. V-site substitutions of $Li_3V_2(PO_4)_3$ by Ni^{2+}, Al^{3+}, Na^{+}, Cr^{3+} have been extensively investigated [20–25] and are considered to be an effective method to improve electrochemical performance. Doping $Li_3V_2(PO_4)_3$ lattice with Cr^{3+} could stabilize the

✉ Xumei Cui
cuixumei@163.com

[1] School of Vanadium and Titanium, Panzhihua University, Panzhihua 617000, China

[2] School of Optoelectronic Technology, Chengdu University of Information Technology, Chengdu 610225, China

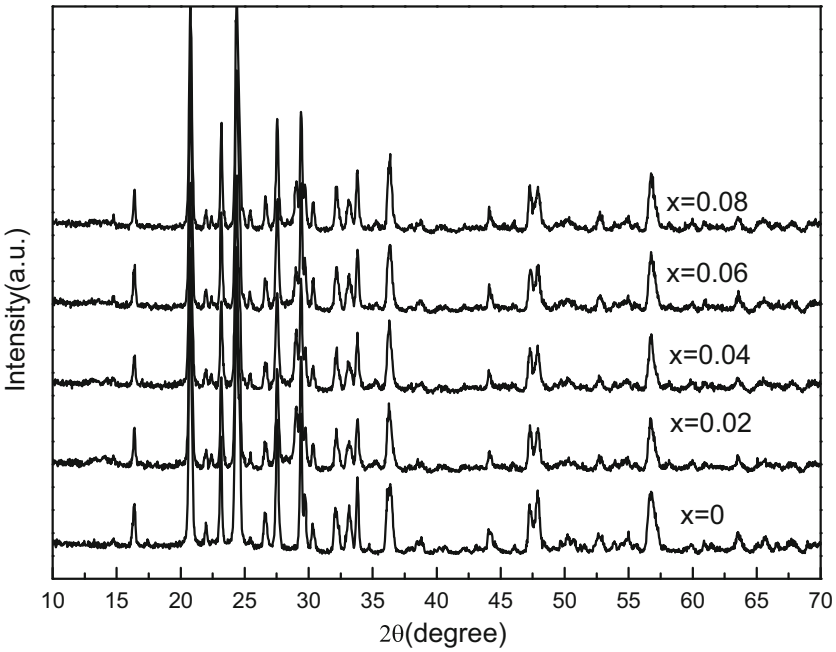

Fig. 1 XRD profiles of $Li_3V_{2-x}Ti_x(PO_4)_3$/C ($x \sim 0$, 0.02, 0.06, and 0.08)

structure of $Li_3V_2(PO_4)_3$, significantly enhancing the specific capacity and cycle life [25].

Ti–Fe codoped samples $Li_3V_{1.9}Ti_{0.05}Fe_{0.05}(PO_4)_3$ have much better high-rate discharge capability and long-term cycling performance than those of $Li_3V_2(PO_4)_3$. However, the electrochemical performance of $Li_3V_{1.9}Ti_{0.05}Mn_{0.05}(PO_4)_3$ is worse than that of $Li_3V_2(PO_4)_3$ [26]. Until now, $Li_3V_2(PO_4)_3$ doped only by Ti^{4+} with carbothermal reduction method have not been studied with voltage range of 3.0–4.3 V [27, 28]. The carbon coating of $Li_3V_2(PO_4)_3$ by citric acid, glucose, maltose, and alginic acid have been reported [29–32]. Because of cheapness, stearic acid as both carbon source and surfactant in preparation of $Li_3V_2(PO_4)_3$ has advantage.

In current work, $Li_3V_{2-x}Ti_x(PO_4)_3$/C ($x \sim 0$, 0.02, 0.04, 0.06, and 0.08) cathode materials were gotten via stearic acid carbon–thermal reduction method [33]. The crystal phase, microstructures, and electrochemical properties of the composites were characterized by XRD, SEM, and electrochemical performance study. And the results showed that Ti doping can not only improve the first discharge specific capacity of $Li_3V_2(PO_4)_3$/C composites but also improve its cycle performance at different rate.

Experimental

Preparation of composite materials

Ti doping $Li_3V_{2-x}Ti_x(PO_4)_3$/C ($x \sim 0$, 0.02, 0.04, 0.06, and 0.08) composite materials were prepared via stearic acid carbon–thermal reduction method, using LiH_2PO_4, V_2O_5, TiO_2, and stearic acid ($CH_3(CH_2)_{16}COOH$, 12.3 wt%) as the raw materials. In which stearic acid acted as the carbon source, chelating agent, and surface active agent [33]. The stoichiometric ratio of Li:V:Ti:P equals to 3:2−*x*:*x*:3. The mixtures were ball milled for 8 h at a rate of 300 r/min with absolute ethanol as a medium and then dried at 80 °C for 12 h. After that, precursor was sintered for 10 h with 750 °C and nitrogen atmosphere, $Li_3V_{2-x}Ti_x(PO_4)_3$/C ($x \sim 0$, 0.02, 0.04, 0.06, and 0.08) composite powders were obtained.

Characterization of composite materials

The crystalline phases of the $Li_3V_{2-x}Ti_x(PO_4)_3$/C ($x \sim 0$, 0.02, 0.04, 0.06, and 0.08) were characterized using X-ray diffraction analyzer (DX-2700) with Cu Kα radiation, and the diffraction angle ranged between 10 and 70° with scan rate of 0.03°/s. The grain morphologies and microstructures of the samples were observed using a scanning electron microscope (FE-SEM, S3400N).

The electrochemical performance of the $Li_3V_{2-x}Ti_x(PO_4)_3$/C ($x \sim 0$, 0.02, 0.04, 0.06, and 0.08) composite materials were tested after the samples were assembled into 2016 coin cells. The cathodes were prepared with $Li_3V_{2-x}Ti_x(PO_4)_3$/C, PVDF, and acetylene black at the weight ratio of 8:1:1, and N-Methylpyrrolidone(NMP) as solvent. After the NMP evaporated, electrodes were punched into a disc with an active area of 1.54 cm^2 and an active loading of ~ 3 mg cm^{-2}. In the 2016 coin cells, lithium metal was used as anode material, and the polypropylene (Celgard2400) was used as the separator membrane. The electrolyte was 1 M LiPF6 with EC+DEC+DMC(volume ratio of 1:1:1) as solvent. And all the cells were assembled in Mikrouna glove box. Constant current charge/discharge measurements were performed with voltage

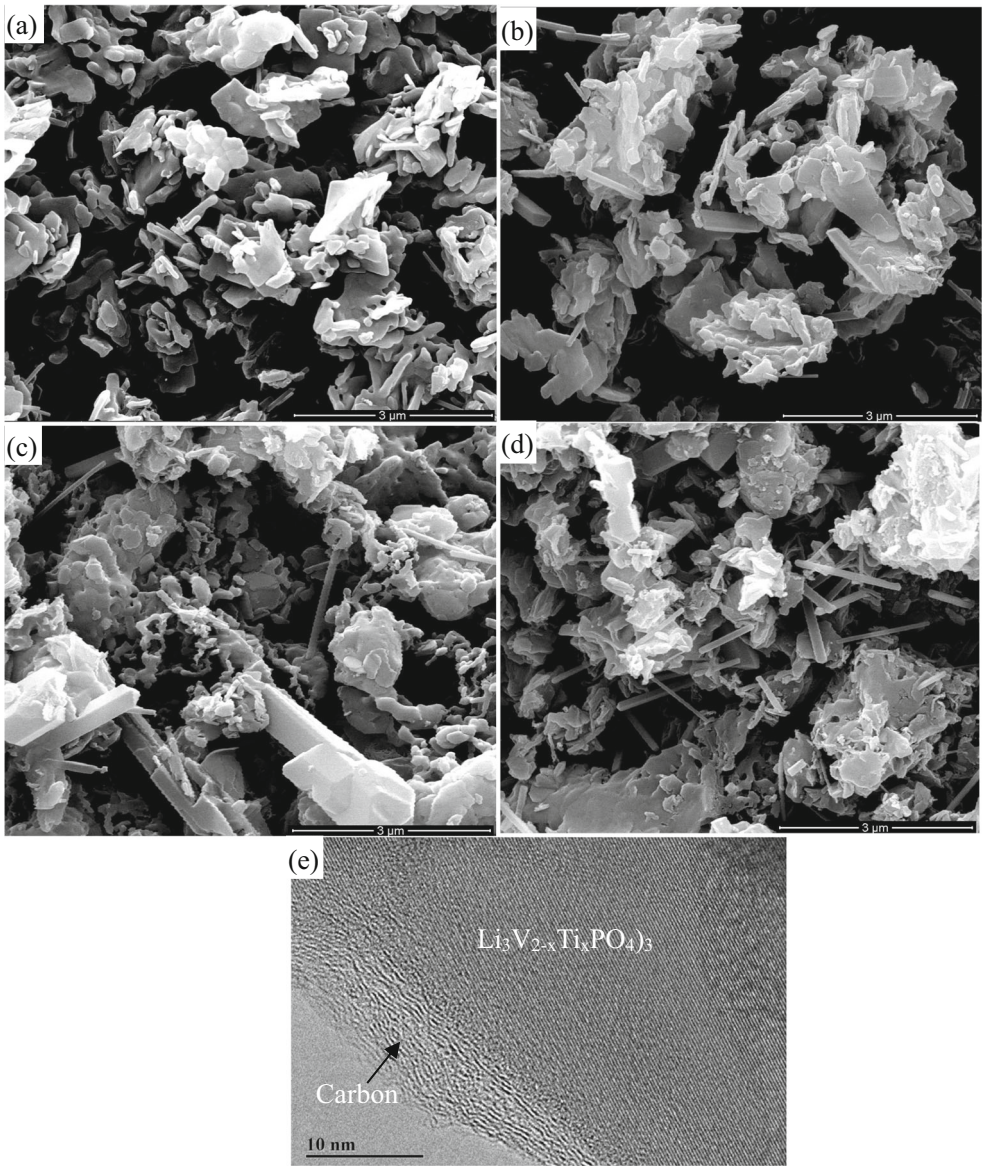

Fig. 2 SEM of the $Li_3V_{2-x}Ti_x(PO_4)_3$/C with **a** $x = 0$, **b** $x = 0.02$, **c** $x = 0.06$, **d** $x = 0.08$; HRTEM of **e** $Li_3V_{2-x}Ti_x(PO_4)_3$/C with $x = 0.06$

window 3~4.3 V at charge–discharge rates of 0.2 C, 0.5 C, 1.0 C, 2.0 C, and 5.0 C on a Land CT2001 testing system (Wuhan, China) [33]. After 60th charge–discharge cycle, the coin cells were subjected to electrochemical impedance spectroscopy (EIS) with CHI660C electrochemical workstation, and the applied frequency range was in the range of 100 kHZ~1 HZ with 5 mV amplitude.

Results and discussion

Structure and morphology characteristics

X-Ray diffraction profiles of the $Li_3V_{2-x}Ti_x(PO_4)_3$/C ($x \sim 0$, 0.02, 0.06, and 0.08) composites are displayed in Fig. 1. As can be seen that the diffraction profiles of the Ti doping composites are very similar to the diffraction profiles of the undoped composite, and no any other extra diffraction reflections can be observed. This shows that atom Ti may enter into the crystal lattice of $Li_3V_{2-x}Ti_x(PO_4)_3$ rather than forms heterogeneous substance. The peaks of the XRD profile almost have the similar positions with standard monoclinic $Li_3V_2(PO_4)_3$ ($P2_1/n$ space group, JCPDS #97-009-6962). And which demonstrates the formation of well crystallized $Li_3V_{2-x}Ti_x(PO_4)_3$/C ($x \sim 0$, 0.02, 0.06, and 0.08). Residual carbon is not detected on the XRD diffraction profiles of the $Li_3V_{2-x}Ti_x(PO_4)_3$/C ($x \sim 0$, 0.02, 0.04, 0.06, and 0.08) composites; its season may be that it has amorphous structure or the carbon film coating on the $Li_3V_{2-x}Ti_x(PO_4)_3$/C ($x \sim 0$, 0.02, 0.06, and 0.08) composites is too thin.

SEM surface morphologies of the pristine composites and Ti doping $Li_3V_2(PO_4)_3$/C composites are given in Fig.

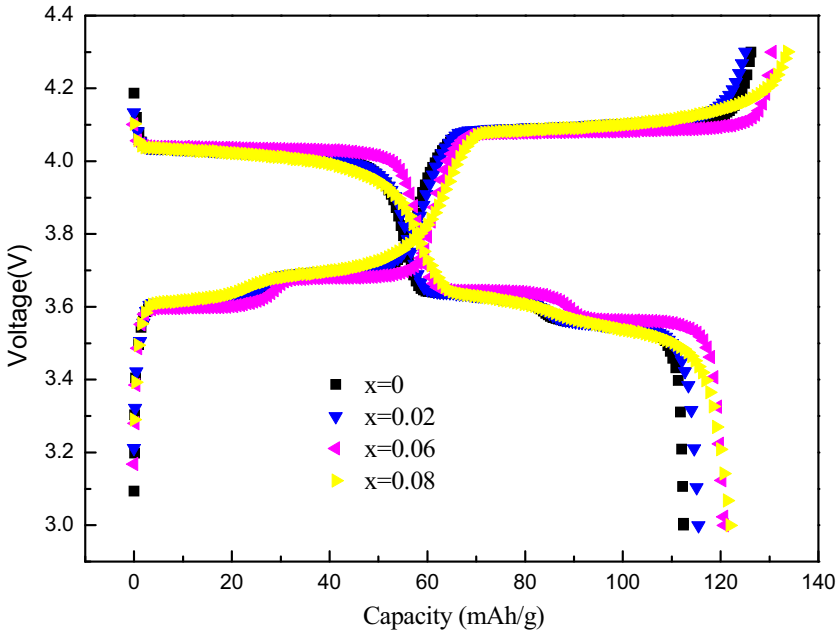

Fig. 3 The first charge–discharge characteristics of $Li_3V_{2-x}Ti_x(PO_4)_3/C$ ($x \sim 0$, 0.02, 0.06, 0.08) electrodes with 0.2 C

2a–d. From the figures, we can obtain that the pristine $Li_3V_2(PO_4)_3/C$ composite is consists of irregular grain sheets of different sizes. After Ti doping of the composites, the $Li_3V_{2-x}Ti_x(PO_4)_3/C$($x \sim 0.02$, 0.04, 0.06, and 0.08) composites have smaller grain size with more nanorods. Also, some holes can be observed from them. The generate of the pore structure can attribute to the combined action of Ti doping and stearic acid, the decomposition of stearic acid is conducive to the generation of the holes. This indicates that Ti doping can reduce the grain size and help for the generation of the holes. The smaller grain size is, the shorter ion diffusion path will become. And thus, Ti doping composites have smaller relative internal resistance, lower self-polarization, and larger surface area, which improves the safety and rate performance of the samples. Nanorods with 60 nm width in $Li_3V_{2-x}Ti_x(PO_4)_3/C$ ($x \sim 0$, 0.02, 0.06, and 0.08) composites also plays a big role in increasing the ion diffusion rate and conductivity. Figure 2e shows the TEM characterization of $Li_3V_{2-x}Ti_x(PO_4)_3/C$ with $x = 0.06$, carbon layer can be

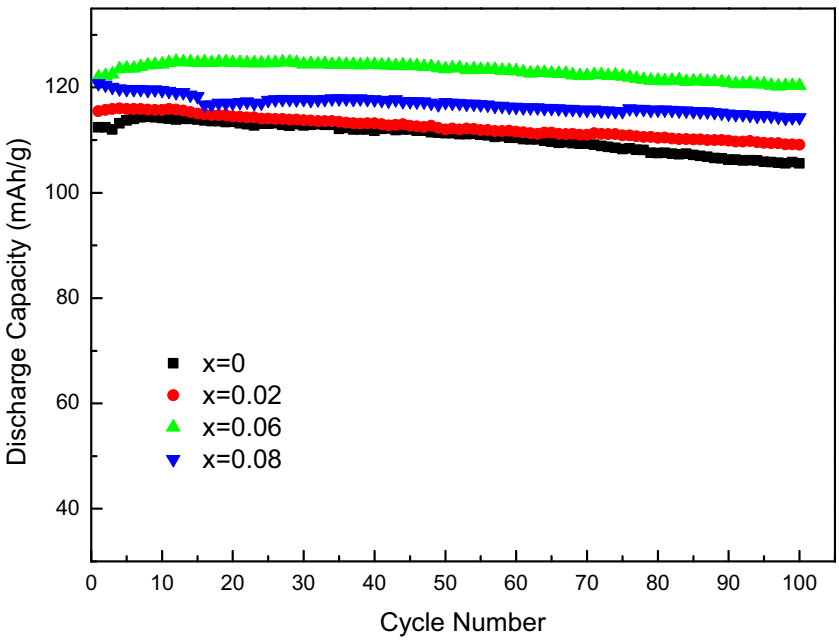

Fig. 4 Cycle performance of $Li_3V_{2-x}Ti_x(PO_4)_3/C$($x \sim 0$, 0.02, 0.06, 0.08) with charge/discharge voltage range 3.0~4.3 V

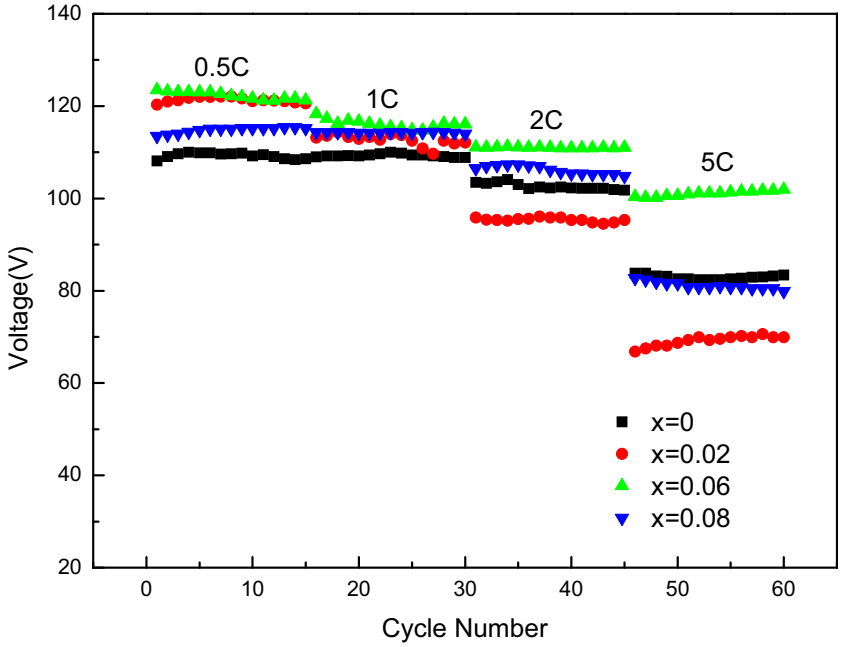

Fig. 5 Cyclic characteristics of $Li_3V_{2-x}Ti_x(PO_4)_3$/C electrodes at different rates with $x \sim 0$, 0.02, 0.06, 0.08

seen at the surface of the LVP, which is beneficial for the electron conductivity improving.

First charge–discharge performance

To determine the electrochemical properties of the $Li_3V_{2-x}Ti_x(PO_4)_3$/C ($x \sim 0$, 0.02, 0.06, and 0.08) composites powder, the charge–discharge curves were measured with a certain current density. Figure 3 presents the first charge/discharge characteristics of all the composites at 0.2 C and 3.0~4.3 V voltage. The charge profile of the pristine composite has three platforms with voltages of approximate 3.60, 3.68, and 4.08 V, respectively. Similarly, there are three discharge platforms during the discharge process at about 3.55, 3.63, and 4.03 V, respectively. Each platform of the charge/discharge curves corresponds to a charge and discharge reaction of lithium ions. There are two charging platforms (3.60 and 3.68 V) for the first lithium ion to extract during charging because of the existence of $Li_{2.5}V_2(PO_4)_3$ ordered phase. After that, the second Li-ion extract, which corresponds a single charging

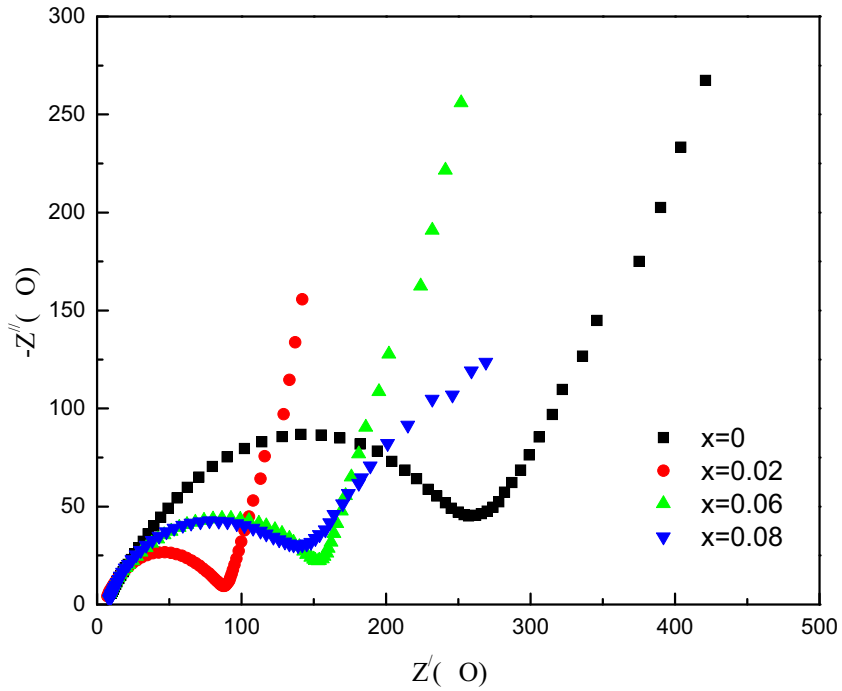

Fig. 6 EIS profiles of $Li_3V_{2-x}Ti_x(PO_4)_3$ samples

platform at about 4.08 V [34]. The three potential platforms correspond to the redox reaction of V^{3+}/V^{4+} pairs.

$Li_3V_{2-x}Ti_x(PO_4)_3/C$ ($x \sim 0$, 0.02, 0.06, and 0.08) samples with different x have the same electrochemical reaction mechanism because they have the similar charging and discharging platform. The voltage platform of the charge and discharge curve varies with the amount of Ti doping. During charging, the voltage of the platforms gradually reduced with x increased, and the sample with x of 0.06 has the lowest voltage platform. During discharging, the voltage of the platforms gradually increased with x increased, and the sample with x of 0.06 also has the highest voltage platform. These phenomena show that $Li_3V_{2-x}Ti_x(PO_4)_3/C$ ($x = 0.06$) powder has the weakest polarization and so it has the highest discharge platform voltage. In addition, it is also apparent that the first discharge performances of the $Li_3V_{2-x}Ti_x(PO_4)_3/C$ ($x \sim 0$, 0.02, 0.06, and 0.08) samples are dependent on the Ti doping amounts. The discharging capacities are approximately 112.4 $mAhg^{-1}$, 115.5 $mAhg^{-1}$, 121.9 $mAhg^{-1}$ and 120.8 $mAhg^{-1}$, respectively. In general, Ti doping samples have higher discharging capacity than undoped sample, the $Li_3V_{2-x}Ti_x(PO_4)_3/C$ sample with $x \sim 0.06$ have the highest discharge platform and discharge voltage, and also the highest discharging capacity. The reason is that Ti doping has been verified to be effective to improve the intrinsic electron transfer conductivity by decreasing the band gap [35] and smaller grain size of $Li_3V_{2-x}Ti_x(PO_4)_3/C$ make the ion diffusion path shorter.

Rate and cycle performance

The cycling characteristics of all $Li_3V_{2-x}Ti_x(PO_4)_3/C$ ($x \sim 0$, 0.02, 0.06, and 0.08) composites at 0.2 C rate are shown in Fig. 4. As can be seen from the figure, that capacity decline of the Ti doping composites is slower than that of the pristine one, and the Ti doping composites show better cycle stability at 0.2 C. For the $x \sim 0$, 0.02, 0.06, and 0.08 samples, 93.95%, 94.46%, 98.69%, and 94.62% of the first discharge capacity was retained after 100 cycles at 0.2 C, respectively. And among them, $Li_3V_{1.94}Ti_{0.06}(PO_4)_3/C$ has the highest capacity retention of 98.69%, and also the maximum specific capacity of 120.3 $mAhg^{-1}$.

To study the rate characteristics of the $Li_3V_{2-x}Ti_x(PO_4)_3/C$ ($x \sim 0$, 0.02, 0.06, and 0.08) composites, all the samples were cycled at four current densities (0.5 C, 1 C, 2 C, and 5 C) with 3.0~4.3 V, and the cyclic results are presented in Fig. 5. The first discharge capacities of the $Li_3V_{2-x}Ti_x(PO_4)_3/C$ ($x \sim 0$, 0.02, 0.06, and 0.08) samples at 0.5 C are approximately 108.1 $mAhg^{-1}$, 120.3 $mAhg^{-1}$, 123.5 $mAhg^{-1}$, and 113.5 $mAhg^{-1}$, respectively. After 15 cycles, discharge capacities of the samples are approximately 108.6 $mAhg^{-1}$, 120.6 $mAhg^{-1}$, 121.5 $mAhg^{-1}$, and 115.2 $mAhg^{-1}$, respectively, and there's basically no reduction in capacity.

After cycled at 0.5 C for 15 times, the composites were cycled at 1 C, 2 C, and 5 C, respectively. Although the discharge capacity of each composite was different, all composites showed good circulation performance. The composites with $x \sim 0.06$ and 0.08 have higher discharge capacity than undoped composites at four current densities (0.5 C, 1 C, 2 C, and 5 C), and the composites with $x \sim 0.06$ have the highest discharge capacity. Therefore, moderate Ti doping can improve cycle and discharge performance with big current rate.

EIS measurements

EIS measurements were performed to analyze the structure of the electrochemical system and the nature of the electrode process with Ti doping over 100 kHz~1 Hz frequency range. Figure 6 shows the EIS profiles of $Li_3V_{2-x}Ti_x(PO_4)_3/C$ ($x \sim 0$, 0.02, 0.06, and 0.08). Each profile consists of a semicircle in the high frequency zone and a slant in the low frequency zone. The semicircle reflects charge transfer reaction resistance, and the slant line reflects Li-ion diffusion resistance in the solid [36]. The depressed semicircles of $Li_3V_{2-x}Ti_x(PO_4)_3/C$ with $x \sim 0.02$, 0.06, and 0.08 are much smaller than the sample with $x \sim 0$, which shows the charge transfer resistance for Ti doping samples is reduced by doping, and it is beneficial for the redox reaction of cathode material and its kinetic process of the reaction. Because Ti doping reduce the grain size, $Li_3V_{2-x}Ti_x(PO_4)_3/C$ with $x \sim 0.02$ and 0.06 have steeper slant lines and it show Ti doping accelerate the solid state diffusion of Li^+, so $Li_3V_{2-x}Ti_x(PO_4)_3/C$ with $x \sim 0.02$ and 0.06 have bigger diffusion coefficients than the pristine $Li_3V_2(PO_4)_3$. And so the rate and cycle performance will be improved by Ti doping, especially for $x \sim 0.06$ samples.

Conclusions

In summary, Ti doping $Li_3V_{2-x}Ti_x(PO_4)_3/C$ ($x \sim 0$, 0.02, 0.06, 0.08) was synthesized by carbon–thermal reduction method. Research showed Ti doping have no effect on the XRD profile of $Li_3V_2(PO_4)_3/C$ composites and there have no extra diffraction reflections at the profiles of the Ti doping samples, which shows that Ti successfully enter into the crystal structure of $Li_3V_2(PO_4)_3$. Ti doping can improve the cycling performance, which is due to its structural stability characteristics. The rate performance is improved by Ti doping with $x \sim 0.06$, which is because its lower charge transfer resistance. And these results can also be attributed to four factors, particle size reduction, more nanorods, more pores in the microstructure of $Li_3V_{2-x}Ti_x(PO_4)_3/C$($x \sim 0.02$, 0.06, 0.08) and the high Li-ion diffusivity of Ti doping $Li_3V_2(PO_4)_3/C$.

Funding information This work was financially supported by the Program for New Century Excellent Talents in University (no. NCET-10-0946), the Science and Technology Innovation Research Team Construction Project of Sichuan Province (no. 2015TD00008), and the Science and Technology Key Project of Sichuan Province (no. 2017JY0038).

References

1. Fergus JW (2010) Recent developments in cathode materials for lithium ion batteries. J Power Sources 195:939–954
2. Lu LG, Han XB, Li JQ, Hua JF, Ouyang MG (2013) A review on the key issues for lithium-ion battery management in electric vehicles. J Power Sources 226:272–288
3. Nam KT, Kim DW, Yoo PJ, Chiang CY, Meethong N, Hammond PT, Chiang YM, Belcher AM (2006) Virus-enabled synthesis and assembly of nanowires for lithium ion battery electrodes. Science 312:885–888
4. Poizot P, Laruelle S, Grugeon S, Dupont L, Tarascon JM (2000) Nano-sized transition-metal oxides as negative-electrode materials for lithium-ion batteries. Nature 407:496–499
5. Scrosati B, Hassoun J, Sun YK (2011) Lithium-ion batteries. A look into the future. Energy Environ Sci 4:3287–3295
6. Wei S, Yao J, Shi B (2017) 1D highly porous Li 3 V 2 (PO 4) 3 /C nanofibers as superior high-rate and ultralong cycle-life cathode material for electrochemical energy storage. Solid State Ionics 305:36–42
7. Chen L, Shaw LL (2014) Recent advances in lithium–sulfur batteries. J Power Sources 267:770–783
8. Crabtree G, Kocs E, Trahey L (2015) The energy-storage frontier: lithium-ion batteries and beyond. MRS Bull 40:1067–1078
9. Ludwig J, Nilges T (2018) Recent progress and developments in lithium cobalt phosphate chemistry- syntheses, polymorphism and properties. J Power Sources 382:101–115
10. Wang L, Zhang L-C, Lieberwirth I, Xu H-W, Chen C-H (2010) A Li3V2(PO4)3/C thin film with high rate capability as a cathode material for lithium-ion batteries. Electrochem Commun 12:52–55
11. Yin SC, Grondey H, Strobel P, Anne M, Nazar LF (2003) Electrochemical property: structure relationships in monoclinic Li3-yV2(PO4)3. J Am Chem Soc 125:10402–10411
12. Zhang X, Liu SQ, Huang KL, Zhuang SX, Guo J, Wu T, Cheng P (2012) Synthesis and characterization of macroporous Li3V2(PO4)3/C composites as cathode materials for Li-ion batteries. J Solid State Electrochem 16:937–944
13. Yoon J, Muhammad S, Jang D, Sivakumar N, Kim J, Jang WH, Lee YS, Park YU, Kang K, Yoon WS (2013) Study on structure and electrochemical properties of carbon-coated monoclinic Li3V2(PO4)3 using synchrotron based in situ X-ray diffraction and absorption. J Alloy Compd 569:76–81
14. Choi SW, Kim DH, Yang SH, Kim MY, Lee MS, Kim HS (2017) The studies of lattice parameter and electrochemical behavior for Li3V2(PO4)3/C cathode materials. J Ind Eng Chem 52:314–320
15. Patoux S, Wurm C, Morcrette M, Rousse G, Masquelier C (2003) J Power Sources 119:278–284
16. Rui XH, Yan QY, Skyllas-Kazacos M, Lim TM (2014) Li3V2(PO4)3 cathode materials for lithium-ion batteries: a review. J Power Sources 258:19–38
17. Sun PP, Zhao XY, Chen RP, Chen T, Ma LB, Fan Q, Lu HL, Hu Y, Tie ZX, Jin Z, Xu QY, Liu J (2016) Li3V2(PO4)3encapsulated flexible free-standing nanofabric cathodes for fast charging and long life-cycle lithium-ion batteries. Nanoscale 8:7408–7415
18. Wang LP, Xu J, Wang C, Cui XM, Li JZ, Zhou YN (2015) A better understanding of the capacity fading mechanisms of Li3V2(PO4)3. RSC Adv 5:71684–71691
19. Hu M, Wei JP, Xing LY, Zhou Z (2013) Improving electrochemical performance of Li3V2(PO4)3 in a thiophene-containing electrolyte. J Power Sources 222:373–378
20. Wu WL, Liang J, Yan J, Mao WF (2013) Synthesis of Li3Ni x V2 −x (PO4)3/C cathode materials and their electrochemical performance for lithium ion batteries. J Solid State Electrochem 17: 2027–2033
21. Zhang Y, Huo QY, Lv Y, Wang LZ, Zhang AQ, Song YH, Li GY, Gao HL, Xia TC, Dong HC (2012) Effects of nickel-doped lithium vanadium phosphate on the performance of lithium-ion batteries. J Alloy Compd 542:187–191
22. Zhong SK, Liu LT, Jiang JQ, Li YW, Wang J, Liu JQ, Li YH (2009) Preparation and electrochemical properties of Y-doped Li3V2(PO4)3 cathode materials for lithium batteries. J Rare Earth 27:134–137
23. Zhong SK, Yin ZL, Liu JQ, Chen QY (2009) Tms 2009 138th annual meeting & exhibition - supplemental proceedings, Vol 2: materials characterization, computation and modeling, pp 229–235
24. Zhong SK, Zhao B, Li YH, Liu YP, Liu JQ, Li FP (2009) Synthesis and electrochemical properties of Cr-doped Li3V2(PO4)3 cathode materials for lithium-ion batteries. J Wuhan Univ Technol 24:343–346
25. Kalaga K, Sayed FN, Rodrigues MTF, Babu G, Gullapalli H, Ajayan PM (2018) Doping stabilized Li3V2(PO4)3 cathode for high voltage, temperature enduring Li-ion batteries. J Power Sources 390:100–107
26. Zhang S, Wu Q, Deng C, Liu FL, Zhang M, Meng FL, Gao H (2012) Synthesis and characterization of Ti–Mn and Ti–Fe codoped Li3V2(PO4)3 as cathode material for lithium ion batteries. J Power Sources 218:56–64
27. Zhong S-K, Wang Y, Wu L, Liu J-Q (2014) Rare Metals 34:586–589
28. Li L, Fan C, Zeng T, Zhang X, Zhang W, Han S (2015) Electrochemical performances of Li 3 V 2-(4/3)x Ti x (PO 4) 3 /C as cathode material for Li-ion batteries synthesized by an ultrasound-assisted sol–gel method. J Alloys Compd 650:136–142
29. Li YJ, Hong L, Sun JQ, Wu F, Chen S (2012) Electrochemical performance of Li3V2(PO4)3/C prepared with a novel carbon source, EDTA. Electrochim Acta 85:110–115
30. Fu P, Zhao YM, An XN, Dong YZ, Hou XM (2007) Structure and electrochemical properties of nanocarbon-coated Li3V2(PO4)3 prepared by sol–gel method. Electrochim Acta 52:5281–5285
31. Fu P, Zhao YM, Dong YZ, An XN, Shen GP (2006) Synthesis of Li3V2(PO4)3 with high performance by optimized solid-state synthesis routine. J Power Sources 162:651–657
32. Hameed AS, Reddy MV, Chowdari BVR, Vittal JJ (2014) Carbon coated Li3V2(PO4)3 from the single-source precursor, Li2(VO)2(HPO4)2(C2O4)·6H2O as cathode and anode materials for Lithium ion batteries. Electrochim Acta 128:184–191
33. Cui XM, Liu TT, Zhang XF, Xiang X (2017) Enhanced electrochemical performance of lithium ion battery cathode Li3V2(PO4)3/C. Ionics 23:3289–3293
34. Deng C, Zhang S, Yang SY, Gao Y, Wu B, Ma L, Fu BL, Wu Q, Liu FL (2011) Effects of Ti and Mg codoping on the electrochemical performance of Li3V2(PO4)3 cathode material for lithium ion batteries. J Phys Chem C 115:15048–15056
35. Yi H, Ling M, Xu W, Li X, Zheng Q, Zhang H (2018) VSC-doping and VSU-doping of Na 3 V 2-x Ti x (PO 4) 2 F 3 compounds for sodium ion battery cathodes: analysis of electrochemical performance and kinetic properties. Nano Energy 47:340–352
36. Choi M, Kim H-S, Moo Lee Y, Choi W-K, Jin B-S (2015) The electrochemical performance of transition metal and graphene added Li 3 V 2 (PO 4) 3 cathode material for Li-ion batteries. Mater Lett 160:194–199